

Supporting information for

Doubly fused *N,N,N*-Iron Ethylene Polymerization Catalysts appended with Fluoride Substituents; probing catalytic performance via a combined experimental and MLR study

Qiuyue Zhang,^{†,‡} Wenhong Yang,[†] Zheng Wang,[†] Gregory A. Solan,^{*,†,§} Tongling Liang[†] and Wen-Hua Sun^{*,†,‡,#}

[†] Key Laboratory of Engineering Plastics and Beijing National Laboratory for Molecular Sciences, Institute of Chemistry, Chinese Academy of Sciences, Beijing 100190, China. E-mail. whsun@iccas.ac.cn; Fax: +86-10-62618239; Tel: +86-10-62557955.

[‡] CAS Research/Education Center for Excellence in Molecular Sciences and International School, University of Chinese Academy of Sciences, Beijing 100049, China.

[§] Department of Chemistry, University of Leicester, University Road, Leicester LE1 7RH, UK. E-mail: gas8@leicester.ac.uk. Tel: +44-116-2522096.

[#] State Key Laboratory for Oxo Synthesis and Selective Oxidation, Lanzhou Institute of Chemical Physics, Chinese Academy of Sciences, Lanzhou 730000, China.

	Table of contents	Page
Figure S1	¹⁹ F NMR spectrum of Fe4 ; recorded in CDCl ₃ at ambient temperature.	S2
Figure S2	1D sequence inverse-gated decoupled ¹³ C NMR spectrum of the polyethylene obtained in entry 8 (Table 2), using Fe4 /MMAO as catalyst (δ C 73.8, tetrachloroethane- <i>d</i> ₂).	S2
Figure S3	1D sequence inverse-gated decoupled ¹³ C NMR spectrum of the polyethylene obtained in entry 8 (Table 3), using Fe4 /MMAO as catalyst (δ C 73.8, tetrachloroethane- <i>d</i> ₂).	S3
Molar ratio determination	Method employed to calculate the proportion of the three types of polyethylene in Figure S3.	S3
Computational part		S3
Table S1	The standardized values of net charge on central metal (<i>Q</i>), open cone angle (θ) and activity for complexes Fe1 – Fe6 .	S4
References	References	S5

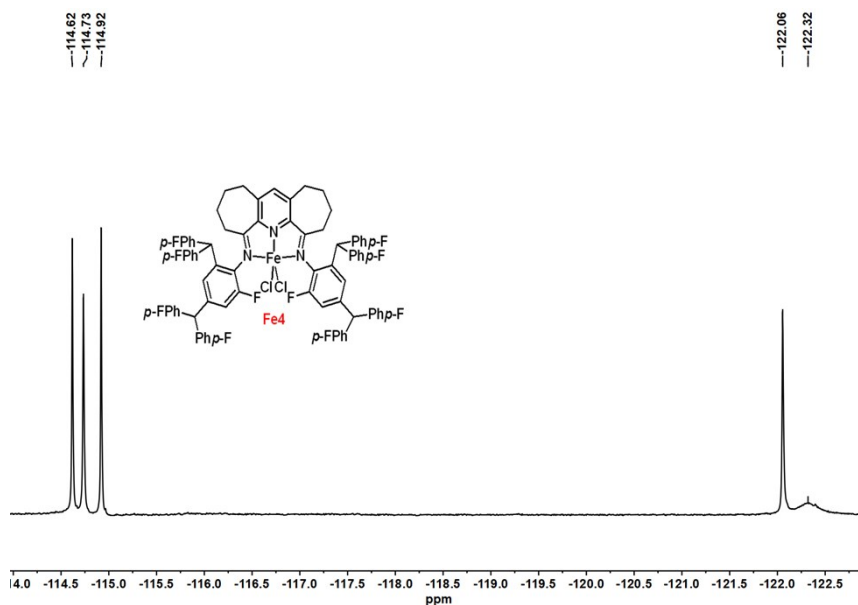


Figure S1. ^{19}F NMR spectrum of **Fe4**; recorded in CDCl_3 at ambient temperature.

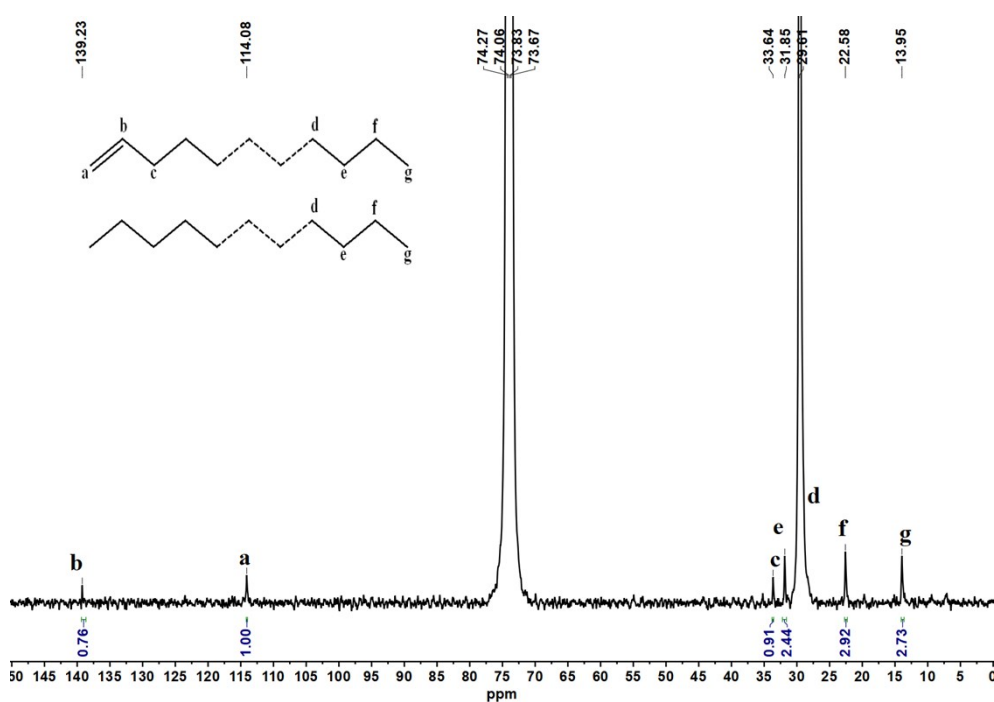


Figure S2. 1D sequence inverse-gated decoupled ^{13}C NMR spectrum of the polyethylene obtained in entry 8 (Table 2), using **Fe4**/MMAO as catalyst (δC 73.8, tetrachloroethane- d_2).

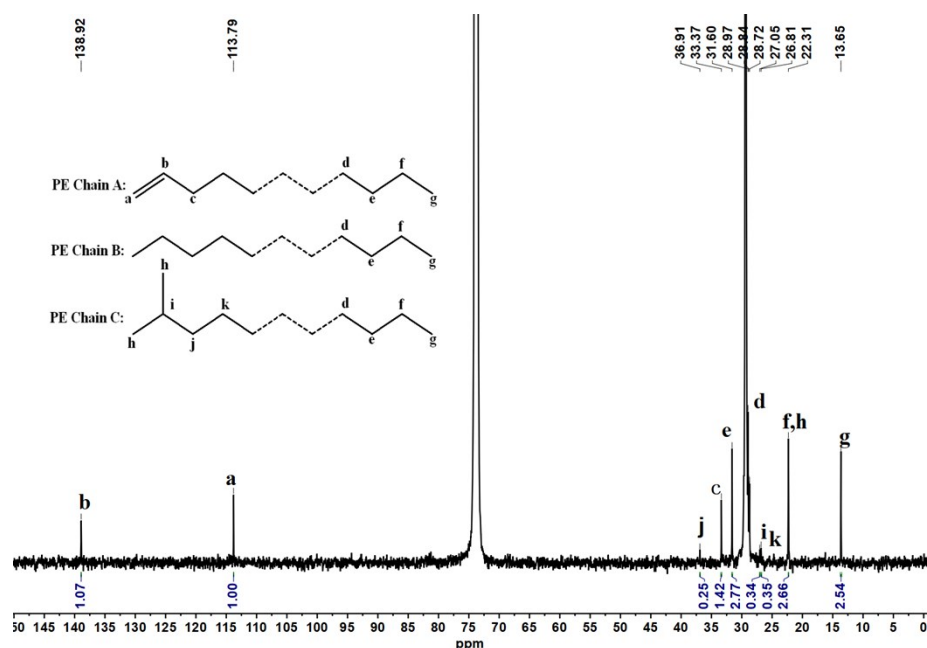


Figure S3. 1D sequence inverse-gated decoupled ^{13}C NMR spectrum of the polyethylene obtained in entry 8 (Table 3), using **Fe4**/MMAO as catalyst ($\delta\text{ C } 73.8$, tetrachloroethane- d_2).

Molar ratio determination: method employed to calculate the proportion of the three types of polyethylene in Figure S3.

By the analysis of the spectrum in Figure S3 above, the integral ratio for peaks C_a to C_g to C_j is 1:2.5:0.3.

Hence, the integration of the C_g peak (2.5) should be split into three parts (1.0 for PE Chain A, 1.2 for PE Chain B and 0.3 for PE Chain C). This means for 1 mole of PE Chain A (1/1), there should be 0.6 moles (as two chain-end CH_3 groups) of PE Chain B (1.2/2) and 0.3 moles of PE Chain C (0.3/1).

Therefore, the molar ratio of PE Chain A to PE Chain B to PE Chain C = **1:0.6:0.3**

By reference to the ^1H NMR spectrum in Figure 14, the ratio of the integrals of H_a to H_g = 2:7.5.

So, it can be inferred that this $H_a:H_g$ ratio = 2:[3 (Chain A) + 3.6 (Chain B) + 0.9 (Chain C)].

Computational Part

To optimize the geometries of six **Fe** complexes, molecular mechanics (MM) [1] calculation has been performed based on our previous reports [2]. Dreiding force field is used in Forcite program package [3]. Since there is no atom type of the central metal and the coordinated nitrogen atoms, we add the corresponding information of bond lengths and bond angles into the force fields on the basis of the experimental crystal data. The convergence tolerances of the force and energy are $0.5 \text{ kcal}\cdot\text{mol}^{-1}\cdot\text{\AA}^{-1}$ and $0.001 \text{ kcal}\cdot\text{mol}^{-1}$, respectively. The cutoff distance of cubic spline is 1.25 nm. To describe electrostatic and van der Waals interactions, atom based Summation and Truncation methods are used, respectively.

In our previous studies, there are seven descriptors from both electronic and steric effects which can reflect the influence of ligand's structure [4]. Herein, we choose two of them, which play the dominant role in determining the catalytic properties of complex, including net charge on central metal atom (Q) and open cone angle (θ). For electronic effect, net charge (Q) is the net charge distribution on central metal atom by QEq method. For steric effect, open cone angle (θ) is calculated in the same manner as previous study [5] by using equation S1.

$$\theta = 360^\circ - \left[\angle C_1 + \arcsin \frac{r_2}{L_2} + \angle D_1 + \arcsin \frac{r_1}{L_1} \right] \quad \text{S1}$$

where $\angle C_1$, $\angle D_1$ and L_1 , L_2 are obtained from the optimized geometry structure of precatalyst, r_1 and r_2 are the van der Waals radius of the outmost atom as shown in Figure S2.

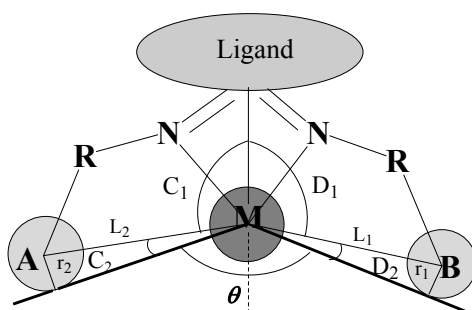


Figure S4. Definition of open cone angle (θ) of complex.

In order to calculate the contribution of each descriptor, Z-Score method is used to standardize the values of descriptors and the catalytic activities [6]. Then the standardized values of the fitting coefficients are obtained to calculate the contribution of descriptor by the equation (S2).

$$\text{Contribution \%} = \frac{\sum_{j=1}^M \frac{|\bar{w}_i \cdot \bar{X}_{ij}|}{\sum_{i=1}^N |\bar{w}_i \cdot \bar{X}_{ij}|}}{M} \times 100\% \quad \text{S2}$$

where, N stands for the number of descriptors, M is the number of the complexes in the present **Fe** system. \bar{X} represents the standardized value of each descriptor, and \bar{w} is the standardized value of fitting coefficient.

Table S1. The standardized values of net charge on central metal (Q), open cone angle (θ) and activity for complexes **Fe1 – Fe6**.

	Fe1	Fe2	Fe3	Fe4	Fe5	Fe6
<i>Q</i>	-0.52	-0.58	-0.61	1.67	-0.73	0.82
<i>θ</i>	-0.29	-0.85	-0.92	0.03	1.82	0.22
<i>Act.</i>	-0.20	-1.05	-1.21	1.16	0.3	0.98

References:

1. NL. Allinger, U. Burkert, *Molecular Mechanics*, (1982) An American Chemical Society Publication. Washington, DC.
2. a) W. Yang, Z. Ma, J. Yi, S. Ahmed, and W.-H. Sun, *J. Comput. Chem.* 40 (2019) 1374–1386; b) W. Yang, S. Ahmed, T. T Fediles, W.-H. Sun, *Catal. Commun.* 132, (2019) 105820–105824; c) W. Yang, T. T Fediles, W.-H. Sun, *J. Comput. Chem.* 41 (2020) 1064–1067.
3. S. L. Mayo, B. D. Olafson, W. A. Goddard, *J. Phys. Chem.* 94 (1990) 8897–8909.
4. a) S. Ahmed, W. Yang, Z. Ma, W.-H. Sun, *J. Phys. Chem. A* 122 (2018) 9637–9644; b) A. A. Malik, W. Yang, Z. Ma, W.-H. Sun, *Catalysts* 9 (2019) 520–527.
5. J. Yi, W. Yang, W.-H. Sun, *Macromol. Chem. Phys.* 217 (2016) 757–764.
6. a) H. P. S. Sachdev, L. Satyanarayana, S. Kumar, R. K. Puri, *Int. J. Epidemiol.* 21 (1992), 916–921; b) S. M. T. Ayatollahi, *Ann. Hum. Biol.* 22 (1995), 151–162.